CANCER BIOLOGY & THERAPY
2019, VOL. 20, NO. 6, 799–811
https://doi.org/10.1080/15384047.2018.1564566

Taylor & Francis
Taylor & Francis Group

RESEARCH PAPER

Check for updates

Inhibition of LINC00994 represses malignant behaviors of pancreatic cancer cells: interacting with miR-765-3p/RUNX2 axis

Xuan Zhu[a,b], Xing Niu[c], and Chunlin Ge[a]

[a]Department of Pancreatic and Biliary Surgery, The First Affiliated Hospital of China Medical University, Shenyang, Liaoning, China; [b]Department of General Surgery, Anshan Hospital, The First Affiliated Hospital of China Medical University, Anshan, Liaoning, China; [c]The Second Clinical Medical School, China Medical University, Shenyang, Liaoning, China

ABSTRACT

Pancreatic cancer exhibits one of the worst prognosis of all human cancers, and it is associated with gene dysregulation. Our microarray results first indicated long intergenic non-protein coding RNA 994 (LINC00994) as an upregulated long non-coding RNA (lncRNA) and miR-765-3p as a downregulated microRNA (miRNA) in pancreatic cancer tissues (Fold change ≥ 2 and $P < 0.05$; three paired samples). To investigate the role of LINC00994 in pancreatic carcinogenesis, a pair of short hairpin RNA (shRNA) was used to stably knock down the endogenous expression of LINC00994 in Panc-1 and AsPC-1 pancreatic cancer cells *in vitro*. We found that LINC00994 silencing inhibited the growth, migration and invasion, and promoted the G1 cell cycle arrest and apoptosis in Panc-1 and AsPC-1 cells. Furthermore, the expression of LINC00994 was negatively correlated with that of miR-765-3p in 10 pancreatic cancer specimens. Runt-related transcription factor 2 (RUNX2), a molecule that contributes to the aggressive behaviors of pancreatic cancer, was herein verified as a novel target for miR-765-3p. Like LINC00994, its expression was elevated in pancreatic cancers. Silencing of LINC00994 and RUNX2 reduced each other's expression in both Panc-1 and AsPC-1 cells. RUNX2 3′UTR and LINC00994 competed to bind miR-765-3p. Additionally, LINC00994-silenced cells regained their aggressive behaviors when miR-765-3p was antagonized, which was accompanied with RUNX2 re-expression. Collectively, our study reveals that LINC00994 contributes to the malignant behaviors of pancreatic cancer cells by preventing miR-765-3p from targeting RUNX2. LINC00994 can be considered as a novel therapeutic target against pancreatic cancer.

ARTICLE HISTORY
Received 3 August 2018
Revised 22 November 2018
Accepted 25 December 2018

KEYWORDS
LINC00994; miR-765-3p; RUNX2; pancreatic cancer; competing endogenous RNA; cancer cell growth; cancer cell mobility

Introduction

GLOBOCAN 2012 estimates that the incidence of pancreatic cancer will reach ~420,000 by the year 2020 worldwide, with a mortality of about 410,000.[1] The newly diagnosed pancreatic cancers in China account for 19.5% of all cases of this cancer.[1,2] The standard of care for resectable pancreatic tumors is surgery followed by anti-cancer chemotherapy, such as gemcitabine-capecitabine combination treatment, and for borderline resectable and unresectable tumors, neoadjuvant therapies provide opportunities to improve the outcome.[3] A very uncomfortable truth in treating pancreatic cancer is that our increasing understanding of the genetic and epigenetic changes has not lead to a significant outcome improvement. Nonetheless, we cannot deny that finding novel molecules involved in pancreatic carcinogenesis will help to improve the therapeutic schedules.

Aberrant gene expression occurs frequently in cancer. It has become evident that not only the protein-coding messenger RNAs (mRNAs), but also the non-coding ones contribute to cancer susceptibility.[4] Non-coding RNAs can be grouped into two major classes on the basis of their size: small non-coding RNAs (< 200 nucleotides) and long non-coding RNAs (lncRNAs; > 200 nucleotides).[4] MicroRNAs (miRNAs), 18–22 nucleotides in length, belong to the small non-coding RNAs, which regulate the expression of their target genes by annealing to the complementary sites on 3′ untranslated regions (3′ UTRs) or on coding sequences.[5] Findings revealing abnormal expression of miRNAs suggest their utility in diagnosis, prognosis, and therapy in pancreatic cancer.[6] Recently, lncRNAs that interact with other RNA species and proteins also gain attention in cancer therapy.[7]

In this study, the expression profiles of lncRNAs and miRNAs in primary cancer and adjacent non-cancer tissues were first obtained from three patients with pancreatic cancer via microarray. Within the differentially expressed non-coding RNAs (Fold change ≥ 2 and P value < 0.05), the upregulated long intergenic non-protein coding RNA 994 (LINC00994) and the downregulated miR-765-3p drew our attention. *Homo Sapiens* LINC00994 RNA is transcribed from *LINC00994* gene which is mapped on chromosome 3p14.1 (*National Center for Biotechnology Information: Nucleotide*). Studies on LINC00994 are scarce. In order to identify what miRNA that may interact with this lncRNA, we raised the screening criteria as fold change ≥ 10 and P value < 0.01. MiR-765-3p, a miRNA with the reduced level in pancreatic

CONTACT Chunlin Ge gechunlin126@126.com Department of Pancreatic and Biliary Surgery, The First Affiliated Hospital of China Medical University, 155 North Nanjing Street, Shenyang, Liaoning 110001, China
Supplemental data for this article can be accessed on the publisher's website.
© 2019 Taylor & Francis Group, LLC

cancer tissues, was the only one met this screening criteria. In different cancers, miR-765-3p's role is different. This miRNA has been demonstrated as an oncomiRNA in hepatocellular carcinoma by Xie et al.[8] and as a tumor suppressor in osteosarcoma by Liang et al. in contrast.[9] Interestingly, miR-765-3p is predicted to bind to LINC00994 at two sites through imperfect complementation. LncRNAs and mRNAs have been described to act as natural miRNA sponges or competing endogenous RNAs (ceRNAs) – they interact with each other by sequestering shared miRNAs.[10] This concept was first proposed by Poliseno and co-workers in 2010,[11] and has been widely reported ever since. The regulatory effects that LINC00994 may have on pancreatic cancer have not been characterized before, and whether it acts as a decoy for miR-765-3p is unknown.

In the present study, Panc-1 and AsPC-1 pancreatic cancer cells with stable low expression of LINC00994 were established, and their tumor behaviors *in vitro* were assessed as well. Our data indicated that LINC00994 silencing inhibited the growth and mobility, and induced apoptosis in pancreatic cancer cells. Further, the changes induced by LINC00994 knockdown in these cancer cells were nearly reversed by miR-765-3p inhibitor.

Materials and methods

Clinical specimens

Non-cancer and cancer tissues were obtained from 10 patients diagnosed with pancreatic cancer in the First Affiliated Hospital of China Medical University. Three sample pairs out of the 10 were subjected to analyses using lncRNA and miRNA microarrays (average age: 63 years old; gender: male). The levels of differentially expressed non-coding RNAs were confirmed with real-time quantitative PCR (Real-time qPCR) in all the paired samples.

Microarrays

Total RNA was extracted from pancreatic tissues with its integrity being analyzed via Agilent Bioanalyzer 2100 (Agilent Technologies). RNA sample with 28S/18S ratio ≥ 0.7 and RNA Integrity Number (RIN) ≥ 7 was subjected to microarray assay after being quantified via NanoDrop ND 2000 (Thermo Scientific). Agilent human miRNA microarray V21 designed to probe a total of 2,549 mature miRNAs and Agilent human lncRNA microrray V5 designed to probe a total of 89,459 lncRNA were used to identify the differentially expressed non-coding RNAs in this study.

Raw data were abstracted by Feature Extraction software V10.7.1.1 (Agilent Technologies), normalized with quantile algorithm, and then analyzed by Genespring software V13.1 (Agilent Technologies). The threshold set for up- and down-regulated lncRNA and miRNAs was a fold change ≥ 2 and a P value ≤ 0.05 (paired student's t test).

Real-time qPCR

Total RNA was isolated from tissues or cells with Trizol. To detect the expression of LINC00994 and Runt Related Transcription Factor 2 (RUNX2), RNA was processed into cDNA with Super M-MLV reverse transcriptase in presence of oligo^{dT} and random primers (BioTeke) according to the manufacture's protocols. To detect miR-765-3p, a stem-loop primer binding to the 3′ portion of miR-765-3p initiated the reverse transcription of this miRNA. Then, the cDNA was mixed with primers for the real-time qPCR (Table 1), Sybrgreen (Solarbio) and 2× Power Taq PCR MasterMix (BioTeke) and analyzed via Exicycler-TM[96] real-time qPCR thermal cycle. Relative RNA levels were calculated through $2^{(-\Delta\Delta Cq)}$.[12] U6 was the control for miRNA-765-3p, while β-actin was the control for LINC00994 and RUNX2.

Table 1. Primer information for real-time qPCR.

	Sequence information
MiR-765-3p	Reverse transcription primer 5′ GTTGGCTCTGGTGCAGGGTCCGAGGTATTCGCACCAGAGCCA ACCATCAC 3′ Real-time qPCR primers Sense: 5′ATCAGTGGAGGAGAAGGAAGG3′ Antisense: 5′GTGCAGGGTCCGAGGTATTC3′
U6	Reverse Transcription Primer 5′ GTTGGCTCTGGTGCAGGGTCCGAGGTATTCGCACCAGAGCCA ACAAAATATGG 3′ Real-time qPCR primers Sense: 5′GCTTCGGCAGCACATATACT 3′ Antisense: 5′ GTGCAGGGTCCGAGGTATTC 3′
LINC00994	Real-time qPCR primers Sense: 5′TCAAGGAGCTGGGATGGA 3′ Antisense: 5′CGAATTGCTGGGAAGAGG 3′
RUNX2	Real-time qPCR primers Sense:5′ TGGACGAGGCAAGAGTTT 3′ Antisense:5′ CTTCTGGGTTCCCGAGGT 3′
β-actin	Real-time qPCR primers Sense: 5′ CTTAGTTGCGTTACACCCTTTCTTG 3′ Antisense: 5′ CTGTCACCTTCACCGTTCCAGTTT 3′

Cell culture and plasmid transfection

Panc-1, AsPC-1 and sw1990 cell lines were obtained from Zhong Qiao Xin Zhou Biotechnology Co.,Ltd., and were cultured in a cell incubator as recommended. No mycoplasma infection was detected in these cell lines. A pair of shRNA targeting LINC00994 (Sense: 5′ GATCCCCAGAAAGTATTATAAGTCTATTCAAGAGAT-AGACTTATAATACTTTCTTTTTT 3′) was synthesized in Sangon, and was constructed into the pRNA-H1.1 vector between BamHI and HindIII (sh-LINC00994) after annealing. Panc-1 and AsPC-1 cells were transfected with negative control shRNA (sh-nc) or sh-LINC00994 via Lipofectamine 2000 (Invitrogen), and cell clones resistant to G418 (Invitrogen; 100 μg/mL for ASPC-1; 150 μg/mL for Panc-1) were selected for the following *in vitro* study. In addition, miR-765-3p mimic and inhibitor were purchased from GenePharma, and were used to transiently transfect pancreatic cancer cells via Lipofectamine 2000.

Full length of LINC00994 was inserted into the pcDNA3.1 vector between HindIII and BamHI sites, and used to transiently transfect sw1990 cells. si-RUNX-2 (NM_001024630; forward 5′ GGUCCUAUGACCAGUCUUAtt3′) was synthesized to transiently transfect Panc-1 and AsPC-1.

Cell growth assay

Control or LINC00994-silenced cells (3×10^3) were seeded in 96-well plates in five duplicates, and the cell proliferation was determined with CCK-8 assay. Twelve, 24, 48 or 72 hrs later, 10 μL CCK-8 (Beyotime) was added into the cell culture, and the absorbance at 450 nm was recorded by a multiscan spectrum.

Scratch assay

Cells grew into a confluence of 100% were subjected to the scratch assay. In brief, the confluent cells were maintained in serum-free culture medium containing 1 μg/mL mitomycin C (Sigma, St. Louis, MO, USA) for 60 min, and then were scratched by a 200 μm-pipette tip. Twenty-four or 48 hrs later, cell micro-images were taken under a light microscope.

Transwell chamber assay

The upper membrane surface of transwell chambers (Corning) was coated with matrigel gel (B&D). Cells (4×10^4 in 360 μL serum-free culture medium) were added into the upper chamber, while the lower chamber filled with culture medium supplemented with 30% FBS. The cell plates were then placed in a standard cell incubator. Twenty-four hrs later, cells invaded through the matrigel gel to the lower membrane surface were stained with 0.5% crystal violet (Amresco). Invaded cells were counted in five random areas in each well, and the data were averaged from three replicates.

Flow cytometry

Apoptotic cells were first marked with Annexin V-FITC/Propidium Iodide (PI) (KeyGene Biotech.), and then analyzed on BD Accuri™ C6 Flow Cytometer (BD Biosciences) according to the manufactures' protocols. For cell cycle, cancer cells were only stained with PI and analyzed on the Flow Cytometer.

Xenograft tumor

Panc-1 (2×10^6) or AsPC-1 (2×10^6) cells were subcutaneously xenografted into nude mice. Tumor formation was monitored every three days since day 10, and the tumors were removed on day 21 from the sacrificed mice.

Dual-luciferase assay

The pmirGLO vector (Promega Corporation) with miR-765-3p target or mismatch sequence was used to evaluate the binding activity of miRNA according to the supplier's protocols. There were two potential bind areas in LINC00994 (NR_033978) and one in RUNX2 (NM_001024630) that were predicted to be bound by miR-765-3p. Three pairs of primers (P1F/R, P4F/R, and P7F/R; see Table 2) were synthesized to amply wild-type (WT) fragments of LINC00994 and RunX2 that bound to miR-765-3p using human cDNAs as templates. Mutant type (MT) fragments of LINC00994 were obtained by performing point nucleotide mutation and overlapping PCR. In short, P1F/P2R and P3F/P1R primers were used to obtain 196-bp and 190-bp fragments, and then these fragments were used as templates in the following PCR assay using P1F/R as primers (LINC00994 MT_647). Similarly, P4F/P5R-P6F/P4R and P7F/P8R-P9F/P7R were used to obtain middle templates, and then P4F/R and P7F/R primers were used to obtain LINC00994 MT_1015 and RUNX-2 MT_1883. These fragments were cloned into a pUM-T vector (BioTeke, Beijing, China) and sequenced. pUM-T plasmids containing correct fragments (2 μg) or pmirGLO vector (2 μg) were digested with Nhe I (2.5 μl) and Sal I (2.5 μl) in a 50-μl reaction system at 37 ℃ for half an hour. Then, WT and MT fragments were inserted into pmirGLO vector between Nhe I and Sal I sites. Thereafter, miR-765-3p mimic (>hsa-miR-765 MIMAT0003945, 5′ UGGAGGAGAAGGAAGGUGAUG3′) and pmirGLO plasmids were co-transfected into the HEK-293 cells. The binding activity of miR-765-3p was quantitatively assessed by calculating the normalized luciferase activity (fly luciferase activity/renilla luciferase activity). The value was compared to that of cells transfected with nc-mimic plus pmirGLO-WT, and was averaged from three replicates.

Western blotting

Cancer cells were lysed with RIPA buffer (Beyotime Biotech.) plus 1% PMSF (Beyotime Biotech.) on ice for 5 min, and then centrifuged (10,000 g) at 4 ℃ for 10 min. Total protein in the supernatant was subjected to western blotting. After separating on SDS-PAGE, protein samples were transferred onto polyvinylidene difluoride membranes (Millipore), and then blocked in skim milk for 1 hrs. Then, the membranes were incubated with rabbit anti-human polyclonal antibody probing bcl-2 (1:200, Boster Biotech), bax (1:5000; ProteinTech) or RUNX2 (1:1000; Bioss Antibodies)

Table 2. Primer information for dual-luciferase assay.

	Name	Sequence (5′ – 3′)	Enzyme site	Size
LINC00994	P1F for WT_647	CAAgctagcTTTGGAGATGAACTGGTATCC	NheI	357 bp
	P1R for WT_647	CACgtcgacGTATTTACAGCTGTTCGGTG	SalI	
	P2R for MT_647	GAGCAACACATCCTCCTCGAAGGAAACTT	-	
	P3F for MT_647	AAGTTTCCTTCGAGGAGGATGTGTTGCTC	-	
	P4F for WT_1015	CGAgctagcTTTCTCCAGTCTCCAGTTCT	NheI	343 bp
	P4R for WT_1015	CAAgtcgacCCTCCAGCACTGGCCAACTT	SalI	
	P5R for MT_1015	TGCTGGGAAGAGCTCCTCGTGGAGGAGGA	-	
	P6F for MT_1015	TCCTCCTCCACGAGGAGCTCTTCCCAGCA	-	
RUNX2	P7F for WT	CAAgctagcGGCAAGGGGCTGTGGAGTTT	NheI	379 bp
	P7R for WT	CAAgtcgacGAGACTCCCAGGCAGGAAG	SalI	
	P8R for MT	GACTTTTCGGGCCTACTAGCAGGGATTG	-	
	P9F for MT	CAATCCCTGCTAGTAGGCCCGAAAAGTC	-	

lower cases, restriction enzyme sites; underline, mutation site

at 4 ℃ overnight, and then with IgG-HRP (1: 5000) for 45 min. Finally, the blots of target proteins were visualized with ECL (Beyotime Biotech.), and compared to that of β-actin.

Data analysis

The whole experiment was performed for three times. Histograms indicated the mean values, and the error bars presented the standard deviation (SD). Data between two groups were analyzed with paired student's *t* test, and data from more than three groups at a single time point were analyzed with one-way ANOVA, followed by Tukey's multiple comparison tests. Data from more than three groups at multiple time points were analyzed with two-way ANOVA followed by Tukey's test. *P* value < 0.05 was considered significant.

Results

Identification of differentially expressed lncRNAs

All analyzed lncRNAs were shown in Volcano plot (Figure 1(a)), and the results showed 26 downregulated and 10 upregulated lncRNAs (fold change ≥ 2 and *P* value < 0.05) in three pancreatic cancers. These differentially expressed lncRNAs were analyzed with unsupervised hierarchical clustering, and the results illustrated that the pancreatic tissue samples could be grouped into two categories: non-tumor and tumor (Figure 1(b)). We next focused on LINC00994, a novel lncRNA that was upregulated in pancreatic cancers.

LINC00994 is required by pancreatic cancer cells for maintaining their aggressive cancer phenotype

The basal levels of LINC00994 in three pancreatic cancer cell lines (sw1990, AsPC-1 and Panc-1) were analyzed with real-time qPCR. AsPC-1 and Panc-1 cells which had higher basal LINC00994 level were subjected to the following RNA interference (RNAi) experiments (Figure 2(a)). An efficient shRNA was used to stably knock down the endogenous LINC00994 in pancreatic cancer cells (Figure 2(b,c)). The G418 resistant cells were plated in six-well plates and cultured until reaching confluent. As shown in sul Figure 1, cancer cells with stable low LINC00994 expression grew much slower than those transfected with sh-nc, but they did not stop growing (sul Figure 1). Results from CCK-8 assay indicated that the growth of LINC00994-silenced cancer cells was much slower than the control cells (Figure 2(d,e)), and data from cell cycle analysis showed that these cells were arrested at G1 stage (Figure 2(f,g)).

Apoptotic cells were marked with Annexin V/PI and analyzed via flow cytometry. The results showed that approximately 16% of Panc-1 cells and 12% of AsPC-1 cells underwent apoptosis when LINC00994 was knocked down (Figure 3(a,e)). The increased bax and decreased bcl-2 in LINC00994-silenced cancer cells confirmed Annexin V/PI results (Figure 3(b,f)). LINC00994 silencing inhibited the growth of xenograft pancreatic tumors, without affecting their formation rate (Figure 3(c,d,g,h)). Moreover, data from wound healing assay illustrated that LINC00994-silenced cells migrated slower to the scratch area than the control cells (Figure 4(a,c)). Results of matrigel-coated transwell assay illustrated that less cells invaded through the matrigel layer when LINC00994 was

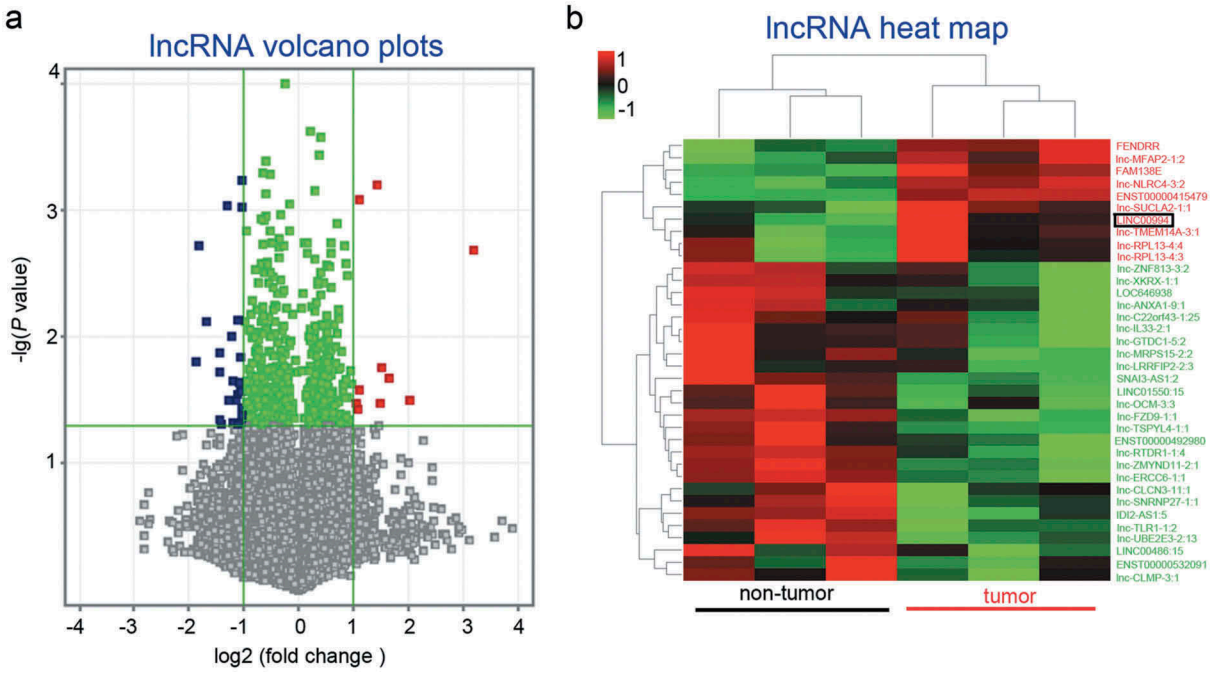

Figure 1. Identification of differentially expressed lncRNA in pancreatic cancer tissues.

LncRNA expression profiles were obtained from pancreatic tumor and non-tumor tissues derived from three patients via microarray. All analyzed lncRNAs were plotted in part (a). Twenty-six downregulated and 10 upregulated lncRNAs (fold change ≥ 2 and *P* value < 0.05) were further analyzed with unsupervised hierarchical clustering, and presented in a heat map (b).

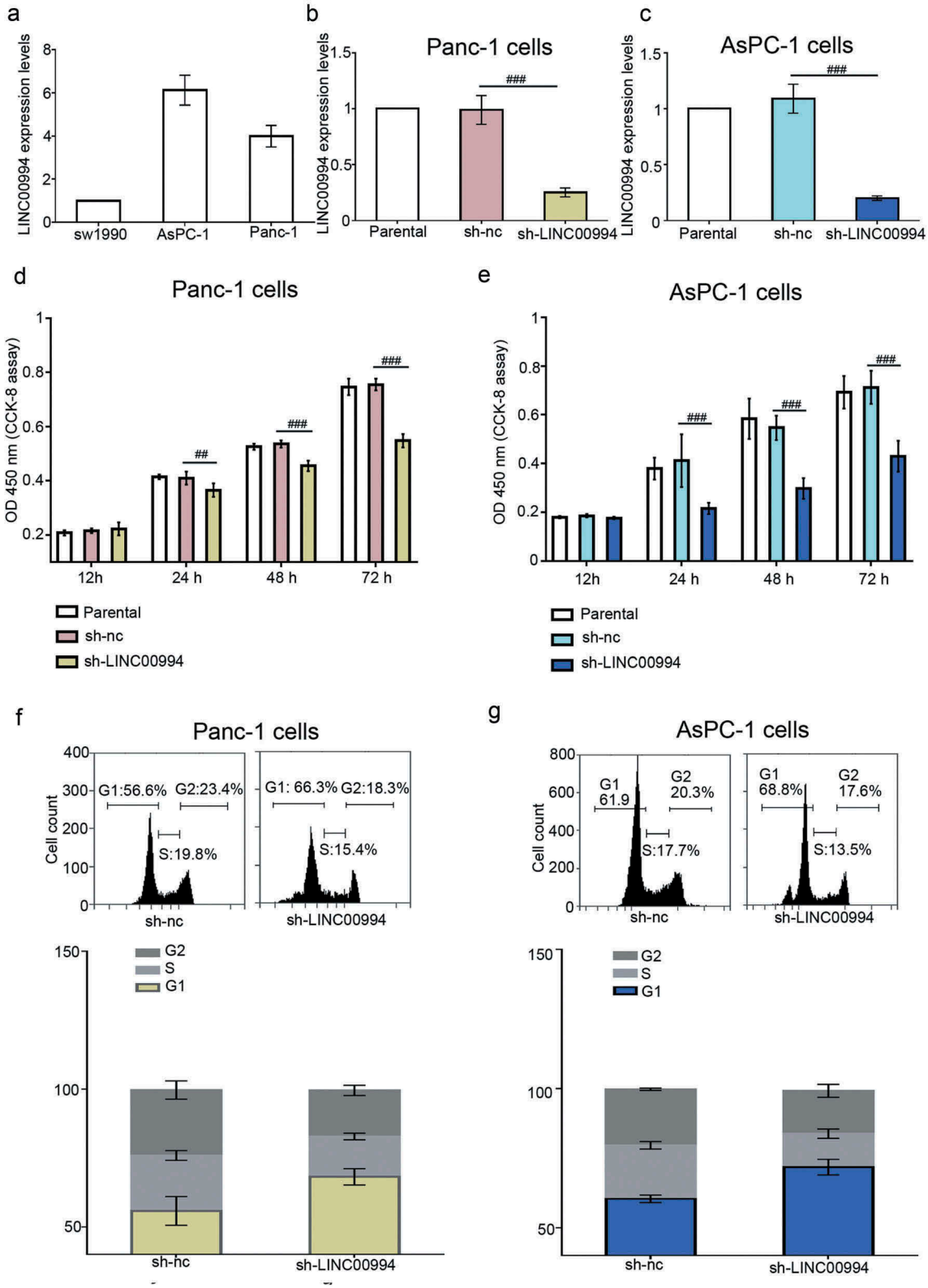

Figure 2. Silencing of LINC00994 inhibits the growth of pancreatic cancer cells.

(a) The basal levels of LINC00994 in sw1990, AsPC-1 and Panc-1 were determined with real-time qPCR. LINC00994 exclusive shRNA was used to stably knock down the endogenous LINC00994 in Panc-1 (b) and AsPC-1 cells (c). (d-e) Cell growth was evaluated by staining the proliferative cancer cells with CCK-8 reagent (N = 5). (f-g) Cell cycle process was determined by staining cancer cells with PI, and analyzed via flow cytometry (N = 3). $^{\#, \#\#, \#\#\#}$ denoted $P < 0.05$, <0.01, and <0.001, respectively. nc, negative control

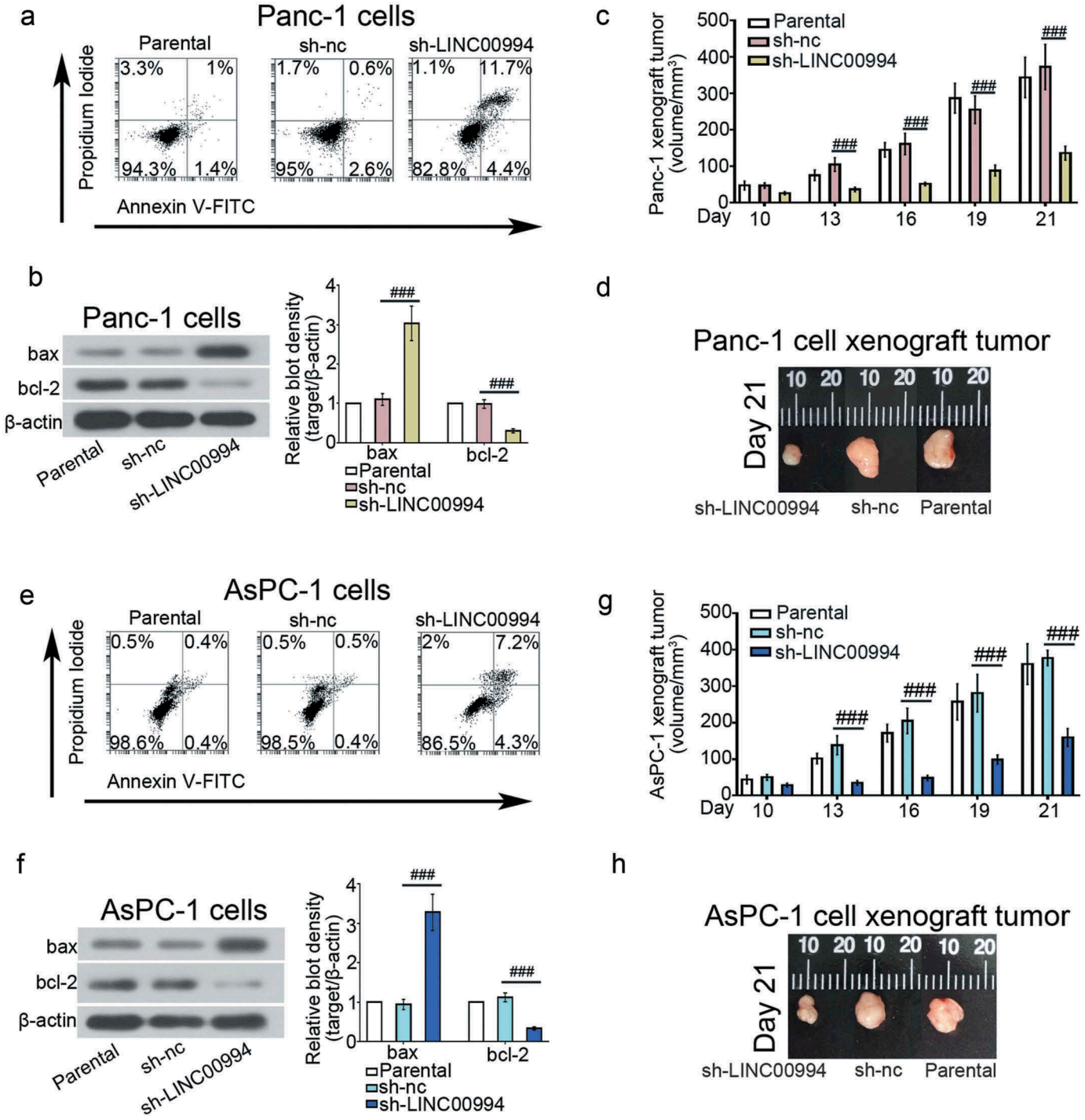

Figure 3. Silencing of LINC00994 promotes apoptosis in pancreatic cancer cells.

(a and e) Apoptotic cells were marked with Annexin V/PI and analyzed via flow cytometry. (b and f) Western blotting was performed to determine the expression levels of bax and bcl-2 in control and LINC00994-silenced cells (N = 3). (c-d and g-h) The growth of xenograft pancreatic tumors were monitored every 72 hrs since day 10 after subcutaneous injection (N = 6). On day 21, nude mice were sacrificed, and tumors were removed. $^{\#, \#\#, \#\#\#}$ denoted $P < 0.05$, <0.01, and <0.001, respectively. nc, negative control

knocked down (Figure 4(b,d)). To avoid the off-target effect of only one shRNA, we additionally evaluated the effect of LINC00994 silencing on pancreatic cells using another shRNA that also effectively suppressed LINC00994. A less aggressive behavior was also observed in pancreatic cancer cells transfected with this shRNA (data not shown). The above data indicated that pancreatic cancer cells with lower LINC00994 expression acquired a less malignant phenotype.

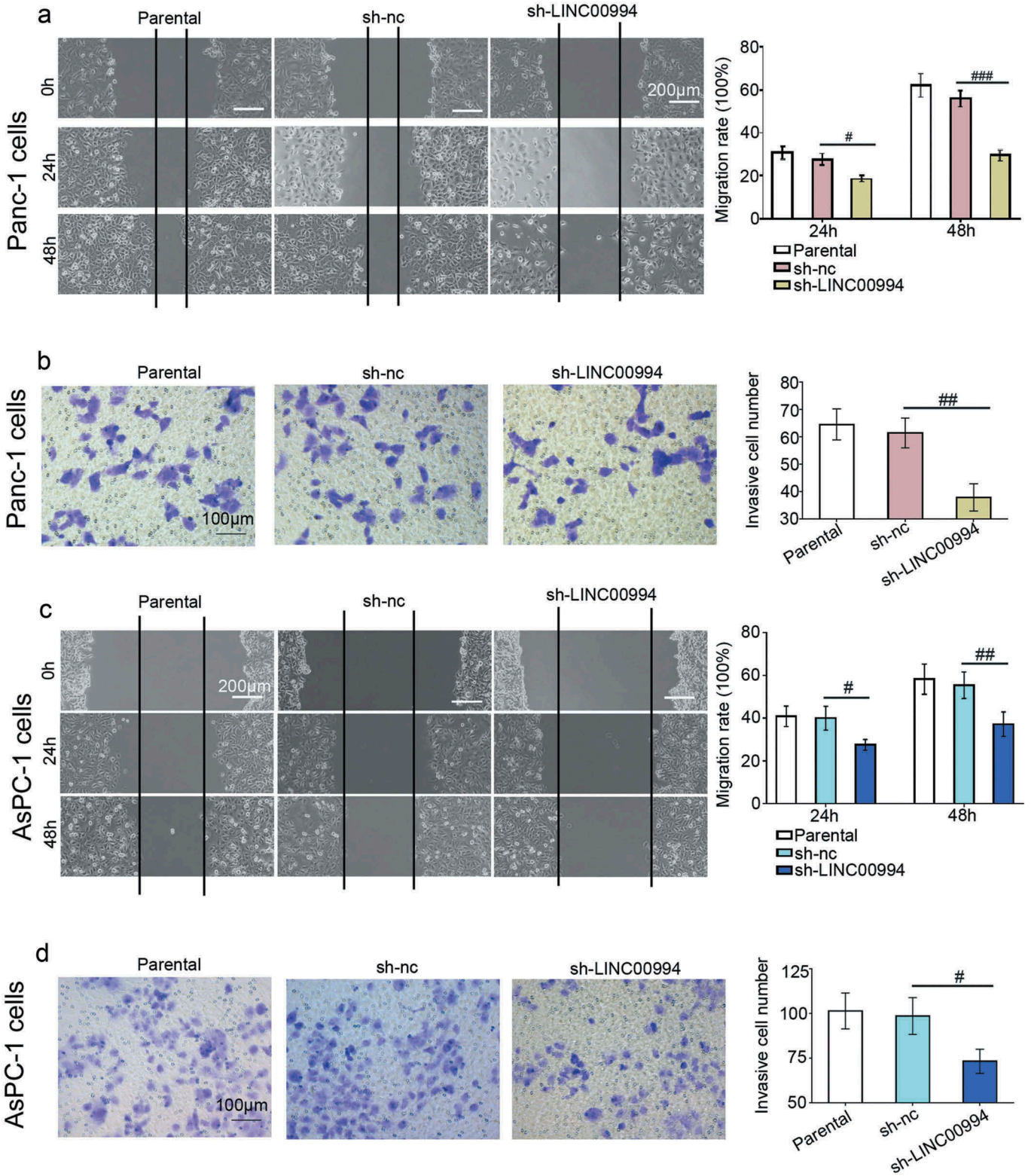

Figure 4. Inhibition of LINC00994 suppresses pancreatic cancer migration and invasion.
(a and c) Wound healing assay was performed to determine the migration rates of Panc-1 and AsPC-1 pancreatic cancer cells (N = 3). (b-d) Matrigel-coated transwell assay was carried out to determine the invasiveness of pancreatic cancer cells (N = 3). $^{\#, \#\#, \#\#\#}$ denoted $P < 0.05$, <0.01, and <0.001, respectively. nc, negative control

Identification of LINC00994-miR-765-3p-RUNX2 axis in pancreatic cancer cells

As lncRNAs have been described to act as natural miRNA sponges,[10] the miRNA expression profile was further analyzed with microarray using the same pancreatic tissues for lncRNA chip. Paired *t* test was used to calculate the *P* values. A higher fold change value indicated a bigger expression alteration, and a smaller *P* value indicated a more significant statistical difference. As shown in Figure 5, nine miRNAs were down-regulated and three were upregulated in pancreatic cancers

(fold change ≥ 2 and *P* value < 0.05). In order to select potential candidate miRNA from the 12 miRNAs, the screening criteria were narrowed down to a fold change ≥ 10 and a *P* value < 0.01.

Only one downregulated miRNA, miR-765-3p (fold change = 23 and *P* value = 0.00089), met the filter criteria. The levels of LINC00994, miR-765-3p and RUNX2 were further analyzed in 10 paired pancreatic samples with real-time qPCR and/or western blotting. We found that the LINC00994 and RUNX2 were upregulated in tumor tissues, while miR-765-3p was downregulated (Figure 5). In addition, LINC00994 levels were negatively correlated with miR-765-3p levels in pancreatic cancers (r = −0.6362) (Figure 5).

By using Gene Expression Profiling Interactive Analysis (GEPIA), we prior analyzed the correlation of LINC00994 with many miR-765-3p potential targets. Interestingly, we found that LINC00994 expression is positively correlated with RUNX2 (R = 0.23, P value = 0.0022, Spearman correlation; sul Figure 2), (a potential target for miR-765-3p).

To demonstrate miR-765 regulates LINC00994 and RUNX2 expression, both miR-765-3p mimic and inhibitor were used to transfect Panc-1 and AsPC-1 cells. The results demonstrated that LINC00994 and RUNX2 expression levels were downregulated in cells transfected with miR-765-3p mimic, but were upregulated in cells transfected with miR-765-3p inhibitor (Figure6(a,c)). By analyzing the sequence details of LINC00994, miR-765-3p, and RUNX2 via miRanda, targetScan and/or RNAhybrid, we found that there were two potential sites within LINC00994 (Figure 6 (d)) and one site within the 3′ UTR of RUNX2 (Figure 6(f)) that may be recognized and bound by miR-765-3p. Both wild and mutant sequences of partial LINC00994 and RUNX2 3′ UTR were inserted into a pmirGLO vector, and transfected with miR-765-3p mimic or nc-mimic into HEK-293 cells. Data from dual-luciferase confirmed that miR-765-3p bound to area 1015 (predominant) and 647 within LINC00994 (Figure 6(e)), and that it also bound to area 1883 within the 3′ UTR of RUNX2 (Figure 6(g)). Furthermore, LINC00994 overexpression plasmid was used

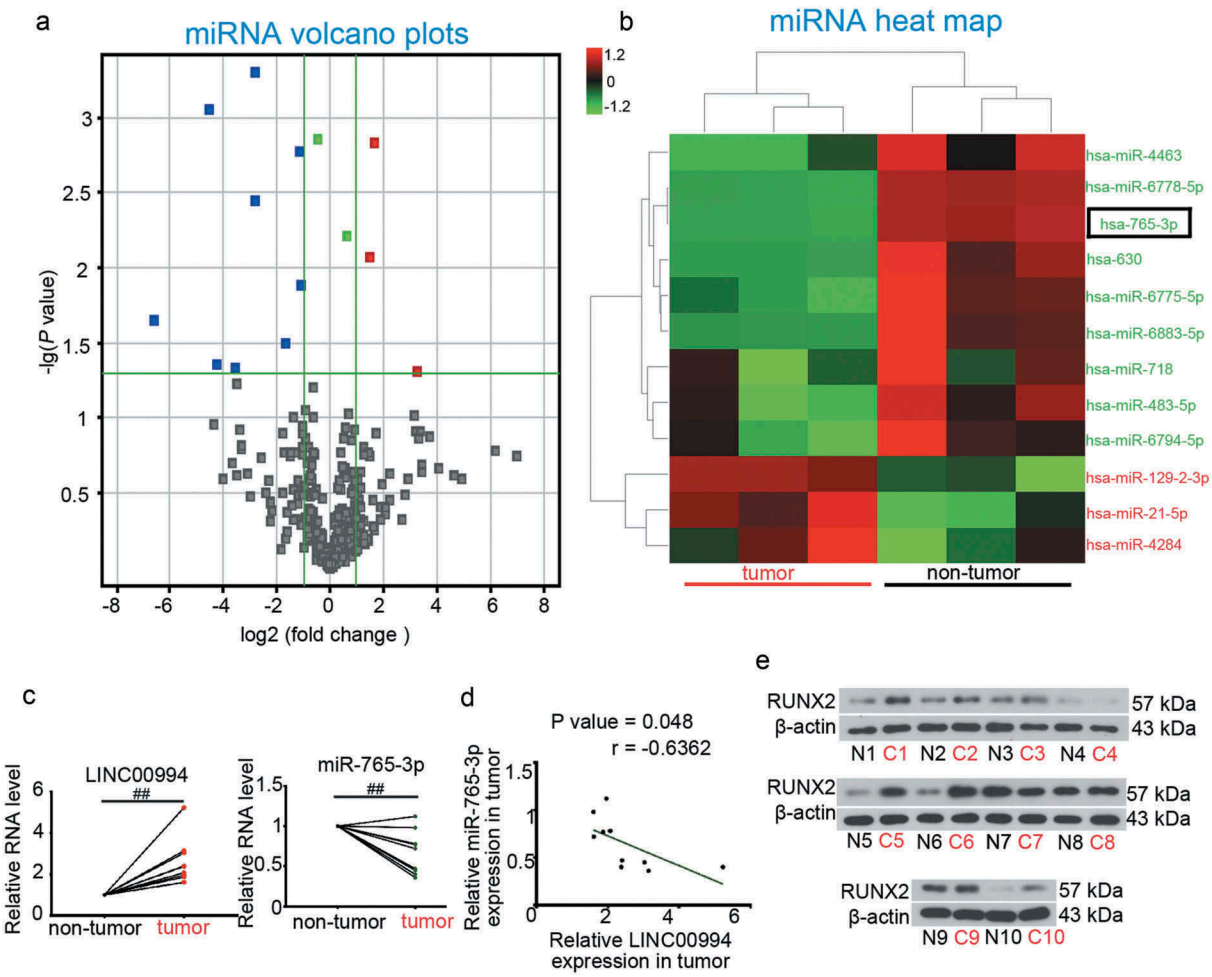

Figure 5. LINC00994 expression is negatively correlated with miR-765-3p in pancreatic cancers.

MiRNA expression profiles were obtained from pancreatic tumor and non-tumor tissues derived from three patients via microarray. All analyzed miRNAs were plotted in part (a). Nine downregulated and three upregulated miRNAs (fold change ≥ 2 and P value < 0.05) were further analyzed with unsupervised hierarchical clustering, and presented in a heat map (b). (c) Real-time qPCR was performed to analyze the levels of LINC00994 and miR-765-3p in 10 paired pancreatic samples. (d) The expression correlation of LINC00994 and miR-765-3p was analyzed with GraphPad prism V7. (e) The protein expression levels of RUNX2, a target of miR-765-3p, were determined with western blotting. $^{\#, \#\#, \#\#\#}$ denoted $P < 0.05$, <0.01, and <0.001, respectively. nc, negative control

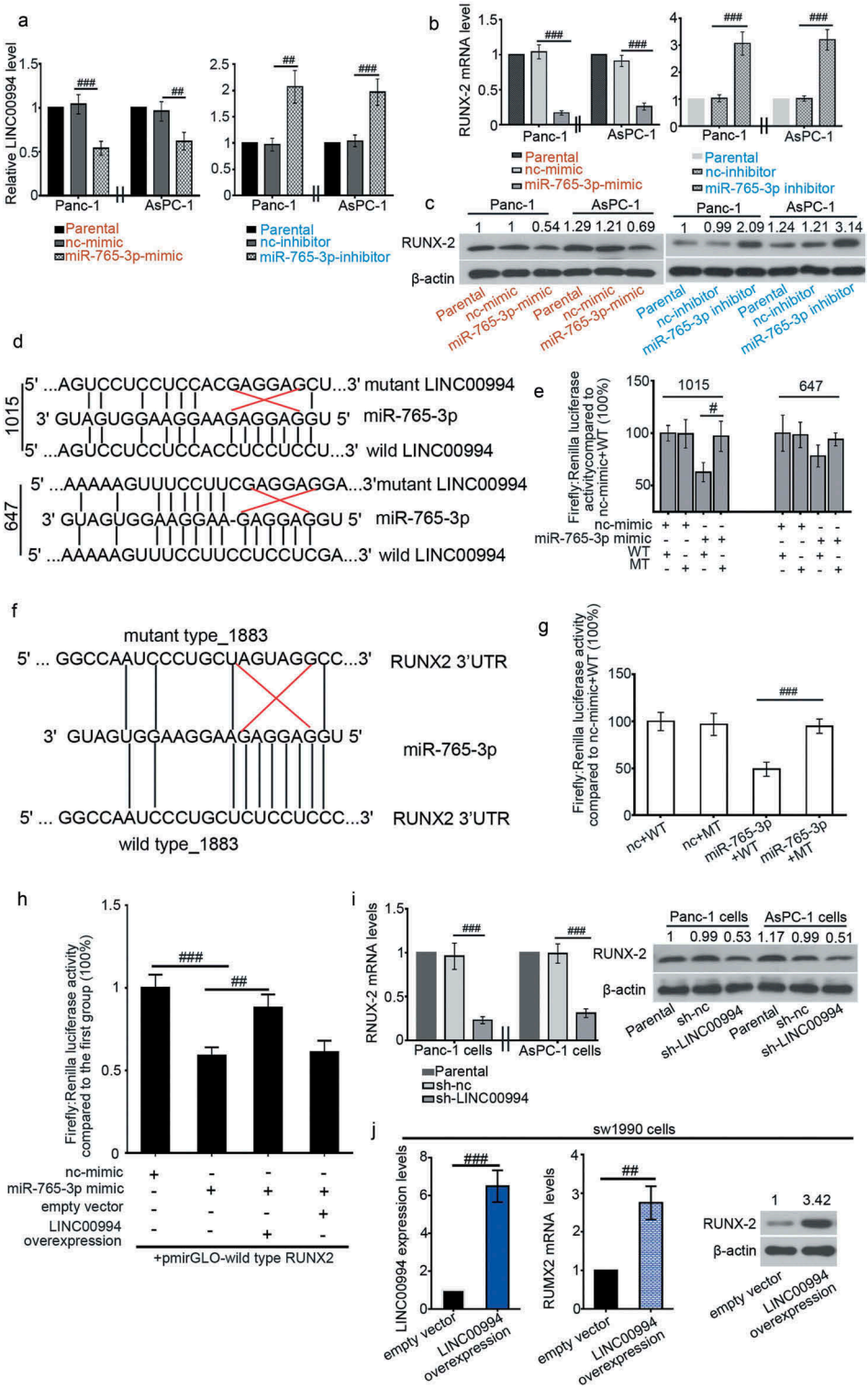

Figure 6. LINC00994 decoys miR-765-3p from targeting RUNX2 in pancreatic cells.

Real-time qPCR was performed to determine the RNA levels of (a) LINC00994 and (b) RUNX2 in Panc-1 and AsPC-1 cells transfected with miR-765-3p mimic or inhibitor (N = 3). (c) Western blotting was performed to determine the protein levels of RUNX2 in these cells. Sequence alignment showed the complementarity between miR-765-3p and (d) LINC00994 and (f) RUNX2. As indicated, both wild (WT) and mutant (MT) fragments were inserted into a pmirGLO vector, respectively. Dual-luciferase confirmed the (e) miR-765-3p-LINC00994 and (g) miR-765-3p-RUNX2 interaction in HEK 293 cells. (h) Dual-luciferase confirmed RUNX2 3′ UTR and LINC00994 competed to bind miR-765-3p. (I) The (left) mRNA and (right) protein levels of RUNX2 were determined with real-time qPCR and western blotting in Panc-1 and AsPC-1 cells, respectively. (j) sw1990 cells were transiently transfected with empty vector or LINC00994 overexpression plasmid, and 48 hrs later, the mRNA levels of (left) LINC00994 and (middle) RUNX2 were determined with real-time qPCR. (right) The protein expression levels of RUNX2 were analyzed with western blotting. $^{\#, \#\#, \#\#\#}$ denoted $P < 0.05$, <0.01, and <0.001, respectively. nc, negative control

to co-transfect sw1990 cells with miR-765-3p or pmirGLO-wild type RUNX2. The results showed that miR-765-3p reduced luciferase activity of pmirGLO-wild type RUNX2, however such effects were weaken after LINC00994 overexpression (Figure 6(h)). These data confirmed that RUNX2 3′UTR and LINC00994 competed to bind miR-765-3p. Knockdown of LINC00994 was performed in Panc-1 and AsPC-1 cells (higher basal LINC00994 expression), and its overexpression was additionally performed in sw1990 cells (lower basal LINC00994 expression). The data showed that RUNX2 expression was positively regulated by LINC00994 (Figure 6(i,j)).

Additionally, Panc-1 and AsPC-1 cells were transfected with si-RUNX2 and si-nc, and the LINC00994 expression levels were determined with real-time qPCR 48hrs later. Results from sul Figure 3 shows that si-RUNX-2 downregulated LINC00994 expression.

LINC00994 sponges miR-765-3p to regulate the malignant behaviors of pancreatic cancer cells

Finally, to confirm that LINC00994 silencing induced a change in the malignant behaviors of pancreatic cancer cells by regulating miR-765-3p, miR-765-3p inhibitor was used to transfect LINC00994-silenced cells. Forty-eight hrs post miR-765-3p inhibitor transfection, the expression of RUNX2 was first analyzed with western blot analysis. Our data indicated that the RUNX2 expression was reduced in LINC00994-silenced cancer cells, but re-expressed when miR-765-3p was antagonized (Figure 7(a,d)). Moreover, cell proliferation was determined with CCK-8 at indicated time points. Our data indicated that the reduction in cancer cell growth was nearly abolished by miR-765-3p inhibitor (Figure 7(b,e)). Cells were transiently transfected by the miR-765-3p inhibitor, a scratch was made on cell surface after refreshing cell culture. Cell images were photographed before and 48 hrs post the scratching. MiR-765-3p inhibitor restored the migration of LINC00994-silenced cells (Figure 7(c,f)).

Discussion

We analyzed the potential interaction of all the differentially expressed lncRNAs with miR-765 with Miranda, a database that can calculate the score and free energy of lncRNA-miRNA interaction. A higher score and a lower free energy indicated a better probability of lncRNA-miRNA interaction. We found that the score for LINC00994-miR-765 interaction was 303, which was within the top three, and the free energy was −43.01 (data not shown). Inspired by the microarray data and the above predictive results, we conducted the present work to investigate whether LINC00994-miR-765-3p interaction contributed to the malignant behaviors of pancreatic cancer cells. We here found that the growth and metastasis of two pancreatic cancer cell lines were suppressed by LINC00994 shRNA. The changes induced by LINC00994 silencing in these cells were less significant when miR-765-3p was antagonized.

Abnormal changes in lncRNA expression are reported to be associated with the carcinogenesis of pancreatic cancer. Several lncRNAs have been identified to be differentially expressed in pancreatic cancer tissues, and can serve as clinical potential biomarkers and therapeutic targets for this cancer. The dysregulated lncRNAs include HOXA Distal Transcript Antisense RNA (HOTTIP),[13] HOX Transcript Antisense RNA (HOTAIR),[14] and Metastasis Associated Lung Adenocarcinoma Transcript 1 (MALAT1).[15] However, except one literature revealing the single-nucleotide polymorphisms of LINC00994 were associated with inflammatory bowel disease,[16] to the best of our knowledge, no previous studies have ever reported the role of LINC00994 in pancreatic cancer. As the microarray data showed an elevation of LINC00994 in pancreatic cancers, we believe that it is interesting to see what consequences the lack of LINC00994 will bring in pancreatic cancer cells. Here, our data for the first time revealed that knockdown of LINC00994 inhibited the proliferation, migration and invasion, and promoted a G1 cell cycle arrest and apoptosis in pancreatic cancer cells *in vitro*.

Genes do not function in isolation, and by interacting with each other, they can group into “networks”. Several previous studies suggest a discrepant regulatory role of miR-765-3p in different types of cancer. Xie et al. found that, compared to the adjacent non-cancerous tissues, miR-765-3p was upregulated in hepatocellular carcinoma tissues, and it acted as a potential oncomiRNA.[8] Later, Liang and co-workers demonstrated that osteosarcoma patients with positive miR-765-3p expression have better overall survival, and this better outcome was associated with the anti-angiogenic effect of miR-765-3p, which suggested miR-765-3p as a tumor suppressor.[9] We here confirmed that the levels of miR-765-3p were negatively correlated to that of LINC00994 in the analyzed pancreatic cancers, and verified their binding by further performing dual-luciferase experiments. We presume that the less aggressive behaviors of LINC00994-silenced cells is associated with miR-765-3p elevation. Results showing that the LINC00994-silenced cells regained their aggressive behaviors when miR-765-3p was antagonized confirmed our hypothesis. Our results also depicted miR-765-3p as a tumor suppressor in pancreatic cancer.

RUNX2 belongs to the RUNX family of transcription factors, and it is well-known for its role in regulating skeletal morphogenesis and osteoblastic differentiation.[17] Of note, RUNX2 has been indicated as a pivotal regulator in carcinogenesis by emerging evidence. RUNX2 was overexpressed in cancer tissues derived from patients with breast cancer,[18] thyroid cancer,[18] myeloma[19] as well as pancreatic cancer.[20] Its aberrant reactivation can promote aggressiveness and metastatic spreading of pancreatic cancer cells.[20] Interestingly, we here verified RUNX2 as a novel and potent target for miR-765-3p in two pancreatic cancer cell lines. In addition to inducing cellular phenotypic change in LINC00994-silencing cancer cells, miR-765-3p inhibitor also provoked the re-expression of RUNX2 in these cells. These data suggest that, in pancreatic cancer cells, LINC00994 and RUNX2 act as competing endogenous RNAs – they interact with each other by sequestering miRNA-765-3p.

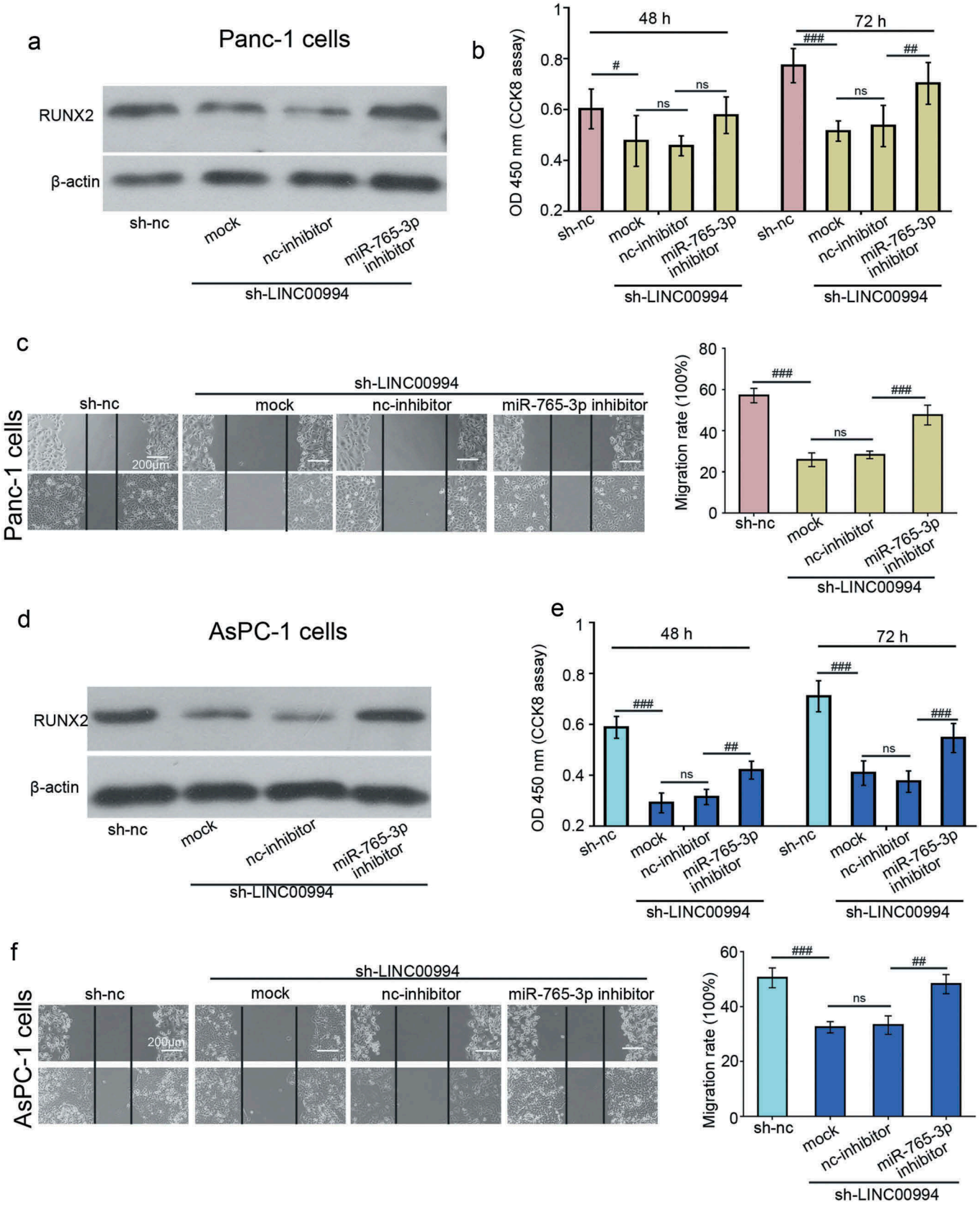

Figure 7. LINC00994-silenced cells regain their aggressive behavior in response to miR-765-3p inhibitor transfection.

LINC00994-silenced Panc-1 and AsPC-1 cells were transiently transfected with nc or miR-765-3p inhibitor, and 48 hrs later, the protein expression levels of RUNX2 were determined with western blotting (a and d). Cells were seeded in 96-well plates 12 hrs post the transfection and their viability was analyzed with CCK-8 assay (N = 5) (b and e). Cell mobility was determined with wound healing assay 48 hrs post the scratching (N = 3) (c and f). $^{\#, \#\#, \#\#\#}$ denoted $P < 0.05$, <0.01, and <0.001, respectively. nc, negative control

Limitations

Our current data revealed a negative expression correlation between LINC00994 and miR-765-3p in pancreatic cancer, which promoted us to investigate how these two non-coding RNAs regulated malignant behaviors of pancreatic cancer cells. However, only 10 pairs of tissue samples were collected for correlation analysis of gene expression in this study. To investigate the association between the dysregulated LINC00994 and miR-765-3p and the aggressive clinical features of pancreatic cancer patients, analyzing more samples is needed.

Pancreatic cancer cell lines with high LINC00994 level may better reflect the real tumor microenvironment than cells with low LINC00994 since LINC00994 was found to be elevated within pancreatic cancers. Thus Panc-1 and AsPC-1 cells with higher basal LINC00994 level were selected for the *in vitro* study. Although we demonstrated that knocking down LINC00994 expression in these cancer cells resulted in a less aggressive cell phenotype, to fully reveal the role of LINC00994, there is also a need to over-express LINC00994 in cells with low LINC00994 level.

RUNX2 is not the only target of miR-765-3p in cancer. Two previous studies showed that miR-765-3p interacted with aminin subunit gamma 2 (LAMC2) and high-mobility group AT-hook 1 (HMGA1) to orchestrate malignant behaviors in cancer cells.[21,22] We also detected the mRNA expression of LAMC2 and HMGA1, two known targets of miR-765-3p, and found that LINC00994 silencing also induced downregulation in them (data not shown). These data suggest that LINC00994 sequesters miR-765-3p from binding to its targets. Notably, miR-765-3p was downregulated in chemoresistant breast cancer tissues.[23] Moreover, silencing of RUNX2 can sensitize pancreatic cancer cells to gemcitabine, the first line of treatment used in most patients with advanced pancreatic cancer.[24,25] These previous findings suggest an involvement of miR-765-3p-RUNX2 axis in chemosensitivity in cancer. As LINC00994 knockdown can suppress RUNX2 by interacting with miR-765-3p, it is possible that LINC00994 also has a role in regulating chemotherapy sensitivity in pancreatic cancer, which requires further exploration.

Conclusion

The present results demonstrate that LINC00994 and RUNX2 are upregulated in pancreatic cancers as compared to non-cancer tissues, while miR-765-3p is downregulated. Silencing of LINC00994 inhibits the growth, migration and invasion, promotes a G1 cell cycle arrest and apoptosis in pancreatic cancer cells *in vitro*. LINC00994-silenced cancer cells regain aggressive tumor behaviors when miR-765-3p is antagonized by the inhibitor. Our work reveals LINC00994/miR-765-3p/RUNX2 as a novel axis that contributes pancreatic carcinogenesis.

Ethics approval and consent to participate

Research involving human subjects was carried out in accordance with the Declaration of Helsinki, and the informed consent was obtained from each participant. Animal study conformed to the policies of the Guide for the Care and Use of Laboratory Animals. This work was approved by the First Affiliated Hospital of China Medical University.

Patient consent for publication

Consent for publication was obtained from each participant.

Disclosure of Potential Conflicts of Interest

No potential conflicts of interest were disclosed.

Funding

This work was supported by the none.

References

1. Ferlay J, Soerjomataram I, Dikshit R, Eser S, Mathers C, Rebelo M, Parkin DM, Forman D, Bray F. Cancer incidence and mortality worldwide: sources, methods and major patterns in GLOBOCAN 2012. Int J Cancer. 2015;136:E359–86. doi:10.1002/ijc.29210.
2. Lin QJ, Yang F, Jin C, Fu DL. Current status and progress of pancreatic cancer in China. World J Gastroenterol. 2015;21:7988–8003. doi:10.3748/wjg.v21.i26.7988.
3. Neoptolemos JP, Kleeff J, Michl P, Costello E, Greenhalf W, Palmer DH. Therapeutic developments in pancreatic cancer: current and future perspectives. Nat Rev Gastroenterol Hepatol. 2018;15:333–348. doi:10.1038/s41575-018-0005-x.
4. Cheetham SW, Gruhl F, Mattick JS, Dinger ME. Long noncoding RNAs and the genetics of cancer. Br J Cancer. 2013;108:2419–2425. doi:10.1038/bjc.2013.233.
5. Adams BD, Parsons C, Walker L, Zhang WC, Slack FJ. Targeting noncoding RNAs in disease. J Clin Invest. 2017;127:761–771. doi:10.1172/JCI84424.
6. Rachagani S, Macha MA, Heimann N, Seshacharyulu P, Haridas D, Chugh S, Batra SK. Clinical implications of miRNAs in the pathogenesis, diagnosis and therapy of pancreatic cancer. Adv Drug Deliv Rev. 2015;81:16–33. doi:10.1016/j.addr.2014.10.020.
7. Lin C, Yang L. Long noncoding RNA in cancer: wiring signaling circuitry. Trends Cell Biol. 2018;28:287–301. doi:10.1016/j.tcb.2017.11.008.
8. Xie BH, He X, Hua RX, Zhang B, Tan GS, Xiong SQ, Liu L-S, Chen W, Yang J-Y, Wang X-N, et al. Mir-765 promotes cell proliferation by downregulating INPP4B expression in human hepatocellular carcinoma. Cancer Biomark. 2016;16:405–413. doi:10.3233/CBM-160579.
9. Liang W, Wei X, Li Q, Dai N, Li CY, Deng Y, Jiang X, Tan X-R, Dai X-Y, Li M-X, et al. MicroRNA-765 enhances the anti-angiogenic effect of CDDP via APE1 in osteosarcoma. J Cancer. 2017;8:1542–1551. doi:10.7150/jca.18680.
10. Tay Y, Rinn J, Pandolfi PP. The multilayered complexity of ceRNA crosstalk and competition. Nature. 2014;505:344–352. doi:10.1038/nature12986.
11. Poliseno L, Salmena L, Zhang J, Carver B, Haveman WJ, Pandolfi PP. A coding-independent function of gene and pseudogene mRNAs regulates tumour biology. Nature. 2010;465:1033–1038. doi:10.1038/nature09144.
12. Livak KJ, Schmittgen TD. Analysis of relative gene expression data using real-time quantitative PCR and the 2(-Delta Delta C(T)) method. Methods. 2001;25:402–408. doi:10.1006/meth.2001.1262.
13. Fu Z, Chen C, Zhou Q, Wang Y, Zhao Y, Zhao X, Li W, Zheng S, Ye H, Wang L, et al. LncRNA HOTTIP modulates cancer stem cell properties in human pancreatic cancer by regulating HOXA9. Cancer Lett. 2017;410:68–81. doi:10.1016/j.canlet.2017.09.019.

14. Kim K, Jutooru I, Chadalapaka G, Johnson G, Frank J, Burghardt R, Kim S, Safe S. HOTAIR is a negative prognostic factor and exhibits pro-oncogenic activity in pancreatic cancer. Oncogene. 2013;32:1616–1625. doi:10.1038/onc.2012.193.
15. Zhou Y, Shan T, Ding W, Hua Z, Shen Y, Lu Z, Chen B, Dai T. Study on mechanism about long noncoding RNA MALAT1 affecting pancreatic cancer by regulating Hippo-YAP signaling. J Cell Physiol. 2018;233:5805–5814. doi:10.1002/jcp.26357.
16. Huang C, Haritunians T, Okou DT, Cutler DJ, Zwick ME, Taylor KD, Datta LW, Maranville JC, Liu Z, Ellis S, et al. Characterization of genetic loci that affect susceptibility to inflammatory bowel diseases in African Americans. Gastroenterol. 2015;149:1575–1586. doi:10.1053/j.gastro.2015.07.065.
17. Ito Y, Miyazono K. RUNX transcription factors as key targets of TGF-beta superfamily signaling. Curr Opin Genet Dev. 2003;13:43–47.
18. Sancisi V, Manzotti G, Gugnoni M, Rossi T, Gandolfi G, Gobbi G, Torricelli F, Catellani F, Faria Do Valle I, Remondini D, et al. RUNX2 expression in thyroid and breast cancer requires the cooperation of three non-redundant enhancers under the control of BRD4 and c-JUN. Nucleic Acids Res. 2017;45:11249–11267. doi:10.1093/nar/gkx802.
19. Trotter TN, Li M, Pan Q, Peker D, Rowan PD, Li J, Zhan F, Suva LJ, Javed A, Yang Y. Myeloma cell-derived Runx2 promotes myeloma progression in bone. Blood. 2015;125:3598–3608. doi:10.1182/blood-2014-12-613968.
20. Kayed H, Jiang X, Keleg S, Jesnowski R, Giese T, Berger MR, Esposito I, Löhr M, Friess H, Kleeff J. Regulation and functional role of the Runt-related transcription factor-2 in pancreatic cancer. Br J Cancer. 2007;97:1106–1115. doi:10.1038/sj.bjc.6603984.
21. Ding J, Yang C, Yang S. LINC00511 interacts with miR-765 and modulates tongue squamous cell carcinoma progression by targeting LAMC2. J Oral Pathol Med. 2018;47:468–476. doi:10.1111/jop.12677.
22. Leung YK, Chan QK, Ng CF, Ma FM, Tse HM, To KF, Maranchie J, Ho S-M, Lau K-M, Yu J. Hsa-miRNA-765 as a key mediator for inhibiting growth, migration and invasion in fulvestrant-treated prostate cancer. PLoS One. 2014;9:e98037. doi:10.1371/journal.pone.0098037.
23. Lv J, Xia K, Xu P, Sun E, Ma J, Gao S, Zhou Q, Zhang M, Wang F, Chen F, et al. miRNA expression patterns in chemoresistant breast cancer tissues. Biomed Pharmacother. 2014;68:935–942. doi:10.1016/j.biopha.2014.09.011.
24. Sugimoto H, Nakamura M, Yoda H, Hiraoka K, Shinohara K, Sang M, Fujiwara K, Shimozato O, Nagase H, Ozaki T. Silencing of RUNX2 enhances gemcitabine sensitivity of p53-deficient human pancreatic cancer AsPC-1 cells through the stimulation of TAp63-mediated cell death. Cell Death Discovery. 2015;1:15010. doi:10.1038/cddiscovery.2015.10.
25. Nakamura M, Sugimoto H, Ogata T, Hiraoka K, Yoda H, Sang M, Sang M, Zhu Y, Yu M, Shimozato O, et al. Improvement of gemcitabine sensitivity of p53-mutated pancreatic cancer MiaPaCa-2 cells by RUNX2 depletion-mediated augmentation of TAp73-dependent cell death. Oncogenesis. 2016;5:e233. doi:10.1038/oncsis.2016.40.